INL/EXT-20-59497
Revision 0

Non-Destructive Postirradiation Examination of the AFC-4C Capsule/ Rodlet 5 Experiment

Nuclear Technology Research and Development

Prepared for
U.S. Department of Energy
Advanced Fuels Campaign

Luca Capriotti,
Idaho National Laboratory
August 2020

SUMMARY

The AFC-4C irradiation test was irradiated at the Idaho National Laboratory Advanced Test Reactor to investigate several different fast reactor fuels that could be used to facilitate ultra-high burnup applications in sodium fast reactors. Several different alloys, fuel geometries, bonding materials, and coating/barrier were tested in ferritic-martensitic HT-9 cladding. The AFC-4C capsule 5 was removed from the reactor at around 8.7 at %HM burnup to begin postirradiation examination.

This report presents and discusses the non-destructive PIE results of the AFC-4C-capsule / rodlet 5, a U-10Zr solid fuel, sodium bonded with HT9 with internal Cr-coating, and its performance is evaluated against the historical fuel performance of previously irradiated fuel from literature.

INTENTIONALLY BLANK

CONTENTS

FIGURES

TABLES

INTENTIONALLY BLANK

ACRONYMS

AFC	Advanced Fuels Campaign
ATR	Advanced Test Reactor
DOE	Department of Energy
EBR-II	Experimental Breeder Reactor II
EFPD	effective full-power days
FCCI	Fuel-cladding Chemical Interaction
FCMI	Fuel-cladding Mechanical Interaction
FFTF	Fast Flux Test Facility
FIMA	Fissions per Initial Metal Atom
HFEF	Hot Fuel Examination Facility
HM	Heavy Metals (atom)
IFR	Integral Fast Reactor
INL	Idaho National Laboratory
KAERI	Korean Atomic Energy Research Institute
LHGR	Linear Heat Generation Rate
MCNP	Monte Carlo N-Particle
MTZ	Mo-Ti-Zr
NRAD	Neutron Radiography Reactor
PGS	Precision Gamma Scanner
PICT	peak inner cladding temperature
PIE	Postirradiation Examination
TRIGA	Training Research Isotope General Atomics
USHPRR	U.S. High-Performance Research Reactor

INTENTIONALLY BLANK

NON-DESTRUCTIVE POSTIRRADIATION EXAMINATION OF THE AFC-4C CAPSULE/RODLET 5 EXPERIMENT

1. INTRODUCTION

A long-term research focus of the US Department of Energy (DOE) Advanced Fuels Campaign (AFC) is to investigate technologies that can allow for increased actinide utilization in nuclear fuel for fast neutron spectrum reactors. This includes both the incorporation of minor actinides into nuclear fuel for transmutation and high utilization of actinides through “ultra high” burnup fuel. This goal is defined as fuel that can reach a burnup of 30-40 percent fissions per initial metal atom (%FIMA) which is higher than what has historically been achieved [1, 2]. Historically, Experimental Breeder Reactor II (EBR-II) Mark III/IIIA/IV driver fuel (U-10Zr fuel with stainless steel 316 or ferritic martensitic steel HT-9 cladding) was qualified to 10%FIMA, but many experimental assemblies and fuel pins achieved higher peak burnup to near 20%FIMA without failure [3]. The motivation of the irradiation tests explored in this work was to screen candidate alloys and forms that could tolerate very high burnup irradiations of up to 30 % FIMA [4,5]. The AFC-4C experiment was irradiated in a prototypic fast reactor spectrum, created by cadmium filtering a thermal neutron dominated spectrum, to investigate fuel performance. Irradiations were performed in the Idaho National Laboratory (INL) Advanced Test Reactor (ATR). The performance of these fuels is compared to the historic performance of U-10Zr [6]. Metallic fuel for fast reactors has a long history that has been reviewed several times in the literature[3,6–10].

These irradiation experiments test several different design variations in metallic fuel for fast reactors with a limited number of samples in addition to testing some variation in irradiation conditions [4]. Because of this, it is difficult to understand fully the complete fuel performance behavior observed in these irradiations. However, it is possible to evaluate this fuel in 4 broad categories. New fuel alloy forms (e.g., U-10Mo, 5Mo-4.3Ti-0.7Zr, -6Zr-4Ta) were tested to evaluate the potential benefit of eliminating constituent redistribution in the fuel. These alloys are single phase from room temperature up to melting. The lack of a phase transition eliminated constituent redistribution and should simplify the modeling of these systems. The second category is U-Zr based fuel. The vast majority of historical experience with U-10Zr is with 75% smeared density sodium bonded fuel. These irradiations stepped outside of that design space to investigate annular fuel bonded without sodium and lower smeared densities. There is interest in removing sodium bonding from fuel to avoid mixed hazardous waste treatment on the back end of the fuel cycle [11]. Low smeared density annular or solid fuel is required to push burnup beyond 20%FIMA because solid fission products begin to fill all available porosity which leads to stress placed on the cladding, resulting in creep of the cladding [6]. The third category is annular fuel, which has been investigated for both U-Mo and U-Zr alloys. The behavior of this fuel is closely connected with the base alloy, but these irradiations have shown the advantage of accurately machining annular fuel to the cladding inner diameter after casting. The fourth category is the addition of an additive, such as Pd, to control lanthanide driven fuel-cladding chemical interaction (FCCI). These irradiations further emphasize the need to balance the amount of additive in the fuel with the major alloying element (Zr or Mo) in order to prevent early life interaction between the fuel and the cladding that can be exasperated by additives.

Finally, in the AFC-4C series, coatings on cladding have been tested to understand their performance in acting as a diffusion barrier to mitigate FCCI.

This report documents the non-destructive postirradiation examination (PIE) performed on AFC-4C capsule/rodlet 5 (abbreviated as C5 / R5) and completed at the Hot Fuel Examination Facility (HFEF) located at the INL Materials and Fuels Complex (MFC). Non-destructive examinations include visual exams, neutron radiography, gamma spectrometry scanning, and dimensional inspection.

2.

SUMMARY OF EXPERIMENT AND IRRADIATION CONDITIONS

2.1 Motivation and Experiment Test Matrix

The AFC 4C irradiation test is an extension of the AFC-3 and AFC-4 irradiation tests to investigate alloys and forms beyond the standard fuel from EBR-II (U-10Zr, 75% smear density, sodium bonded solid fuel). The test matrix for AFC-4C is shown in Table 1 AFC-4C repeated some of the alloys already explored in AFC-4A [12] but at an extended burnup.

The irradiated alloys were either U-10Zr, U-Mo-Ti-Zr or, U-6Zr-6Ta. The two rodlets with U-10Zr alloys were in annular form (helium bonded) and solid form (sodium bonded), both also testing a new HT-9 with Cr coating to protect / mitigate against FCCI. Helium-bonded annular fuel was explored to remove the sodium bond from the fuel. The sodium bond creates an additional complication on the back end of the fuel cycle, forcing fuel to be treated prior to disposal in a once-through fuel cycle.

The Mo-Ti-Zr (MTZ) alloy sought to keep the fuel single phase during irradiation, thus preventing constituent redistribution, while still providing the FCCI benefits that U-Zr alloy fuels enjoy over U-Mo alloy fuels. The additive Pd was also explored in this system. A more detailed examination of this fuel system is provided in [12].

Finally, addition of Ta also was meant to prevent constituent redistribution in the fuel, potentially simplifying fuel modeling.

Table 1. AFC-4C test matrix.

Rodlet ID	Fuel alloy	Cladding type	Fuel Form	Bond Material	Nominal Smear Density	Fuel Outer Diam. (mm)	Fuel Inner Diam. (mm)	Fuel Height (mm)
4C-R1	U-10Zr	HT-9 w/ Cr coating	Annular	Helium	60%	4.93	3.10	38.1
4C-R2	U-6Zr-4Ta	HT-9	Solid	Sodium	75%	4.27	N/A	38.1
4C-R3	U-5Mo-4.3Ti-.7Zr	HT-9	Solid	Sodium	75%	4.27	N/A	38.1
4C-R4	U-5Mo-2Pd-4.3Ti-.7Zr	HT-9	Solid	Sodium	75%	4.27	N/A	38.1
4C-R5	U-10Zr	HT-9 w/ Cr coating	Solid	Sodium	75%	4.27	N/A	38.1

2.2 Irradiation Capsule Design Cadmium Shroud Description/Approach

The basic design of the AFC-4 irradiation experiments is illustrated in Figure 1. The fuel is irradiated in a Cd shroud (Figure 1a) to create a radial power profile that is prototypic of fast reactor conditions [13]. The validity of the technique has been evaluated previously and is documented in the Spectrum Comparison Report [14]. The AFC-4C alloys were formed by mixing appropriate quantities of metals in an arc melter. The alloys were homogenized through a series of several melts. The alloys were then gravity cast into quartz molds using the arc melter. The annular fuel molds contained an inner quartz core. After casting, the molds are removed by breaking the quartz off the outside of the cast pins. For the annular pins, the inner quartz core was removed from the cast pin by drilling. The outside of the annular slugs was machined to the desired outer diameter. The fuel slugs were then cut to length.
For each rodlet, the fabricated fuel is placed inside HT-9 cladding with an inner diameter of 4.93 mm and an outer diameter of 5.84 mm. For rodlets 1 and 5, the HT-9 cladding tubes incorporate an approximately

20 µm Cr coating on the cladding inside diameter. These rodlet tubes were sent to the Korean Atomic Energy Research Institute (KAERI) for coating application [15,16]. After coating, the tubes were sent back to INL where each was cut to final length and dimensionally inspected.

The sealed rodlets are then placed inside a stainless steel 316 capsule as shown in Figure 1b. The capsule provides temperature control across the gap between the rodlet and the capsule and is the primary safety barrier between the experiment and the ATR coolant.

The fabrication of AFC-4C is specified in INL document SPC-1955 [17] documented in project files as the AFC-4C As-Built Data Package and ECAR-3121 [18] for the rodlets and the capsules.

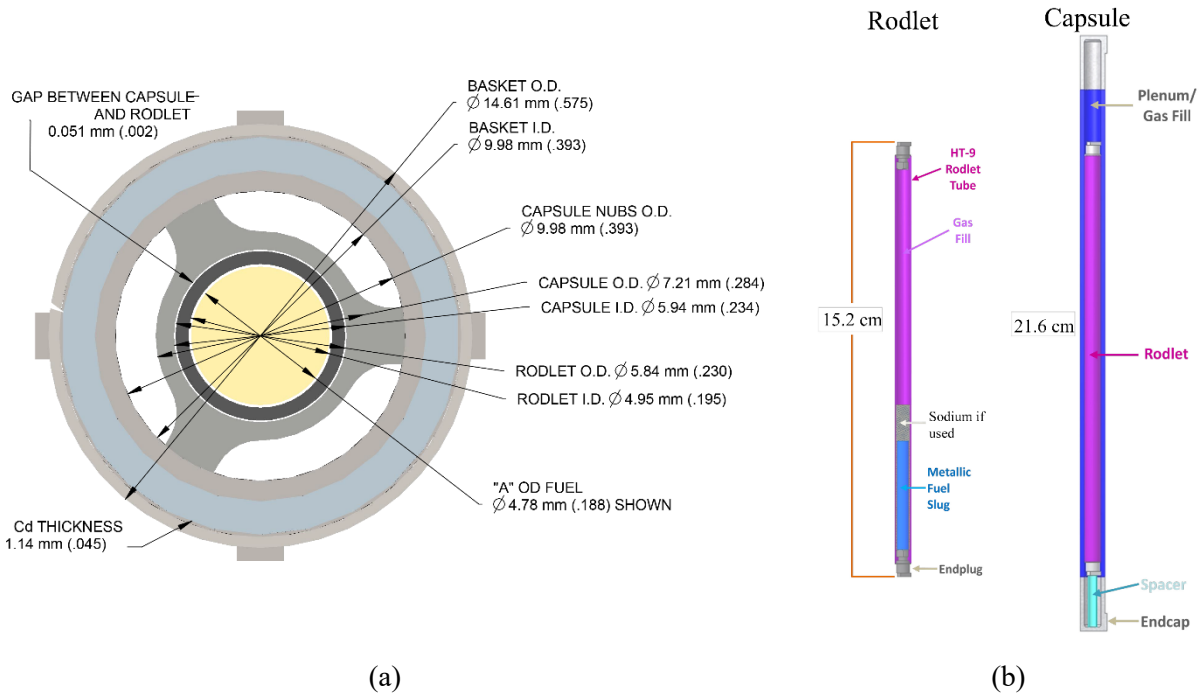

(a) (b)

Figure 1. (a) AFC-3/4 Cross section with Basket, Capsule, Rodlet, and fuel, (b) Typical configuration of AFC rodlet and capsule.

2.3 AFC-4C Irradiation History

All the AFC-4C capsules were placed in the reactor during the same cycles. Irradiation began on February, 2016 in ATR Cycle 158B, the description of the different cycles are reported in Table 2. AFC-4C-C5 was removed after completion of ATR Cycle 166B after 507 EFPD. The calculated accumulated fission density on this rodlet was 3.173E+21 fiss/cm^3 and calculated burnup 8.715 at% HM.

Table 2. Irradiation History of AFC-4C-C5/R5.

Cycle	Start Date	End Date	EFPD	AFC-4C capsule 5 Cumulative EFPD
158B	2/09/2016	04/01/2016	51.4	51.4
160A	9/16/2016	11/08/2016	52.9	104.3
160B	12/19/2016	02/23/2017	60.1	164.4
162A	10/06/2017	12/07/2017	61.9	226.3
162B	2/16/2018	03/29/2018	38.5	264.8
164A	6/10/2018	08/17/2018	54.9	319.7
164B	9/18/2018	01/17/2019	64.1	383.8

166A	7/25/2019	10/06/2019	62.5	446.3
166B	11/09/2019	01/10/2020	61.2	507.5

The as-run neutronic and thermal irradiation histories for the capsules were calculated by combining the results of neutronic and thermal analysis. The heat generation and linear heat generation rate (LHGR) is calculated using whole ATR core Monte Carlo N-Particle (MCNP 6.0) simulations coupled with ORIGEN for depletion. The recorded ATR power history from each cycle and the initial ATR core loading are used as inputs to these simulations. The heat generation rates are then supplied to a finite element analysis code (Abaqus) to calculate the temperatures in the capsule. The axial variation in power and temperature is relatively low. For the fuel documented in this work, fuel performance can largely be tied back to the inner cladding temperature. The inner cladding temperature adjacent to the fuel slug is no more than ±20°C from the peak inner cladding temperature (PICT). Through the finite element analysis, it was possible to generate a relationship between LHGR and PICT [19]. The LHGR varies directly with the ATR lobe power for the location of the capsule. The ATR lobe power history has been converted to LHGR history for each capsule and further converted to the PICT history for the capsule. The PICT is plotted against EFPD in ATR in Figure 2.

AFC-4C-R5 experienced the first part of irradiation at PICT around 530-570 °C, and then in the last cycles, milder conditions with PICT ranging from 480-510 °C.

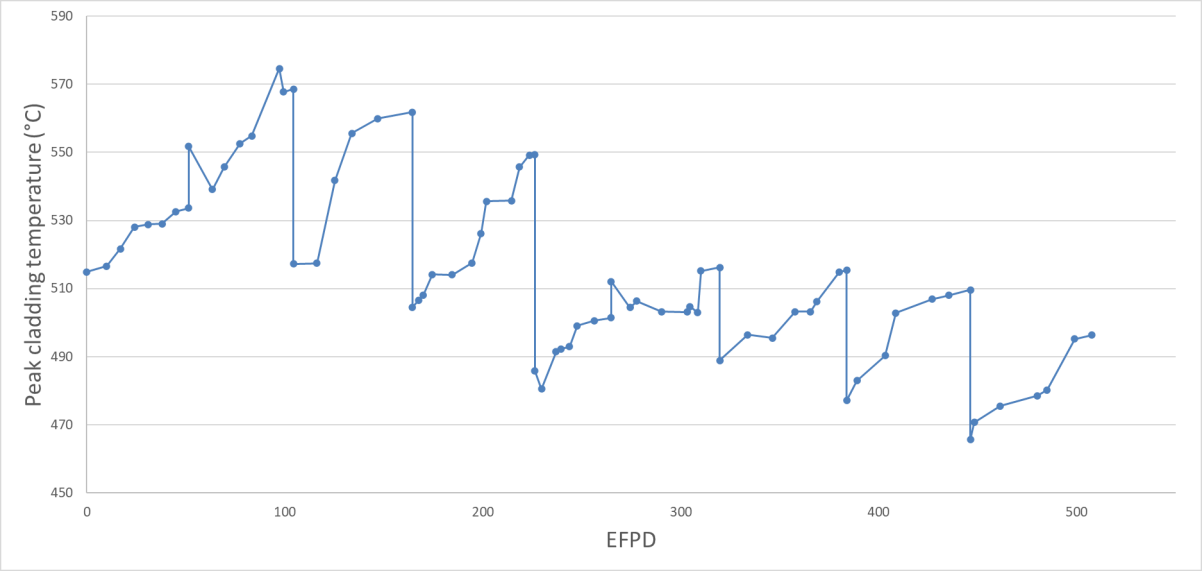

Figure 2. PICT history for AFC-4C-R5 experiments.

3. NON-DESTRUCTIVE PIE RESULTS OF AFC-4C CAPSULE / RODLET 5

Non-destructive postirradiation examination (PIE) results from the examination of AFC-4C C5/R5 are summarized in the following section. These examinations included visual, neutron radiography, dimensional inspection, gamma-ray spectrometry. These exams evaluate the engineering scale performance of the fuel and can be related to the phenomenological performance of the fuel as well.

3.1 Visual exams

Visual exams are currently performed by through-window photography. The capsule and rodlet are placed on a neutral background fixture with a scale. The fixture is held in place by one of the in-cell electro-mechanical manipulators. After the initial photograph is taken, the capsule / rodlet is rotated and

at least a second angle is taken. Figure 3 presents a photo of the capsule and Figure 4 of the rodlet.

The visual exam of the rodlet did not reveal any obvious flaws in the cladding. There are no obvious visual defects apparent in the rodlet, and only some discoloration can be noticed on the fuel region (right hand side in Figure 4).

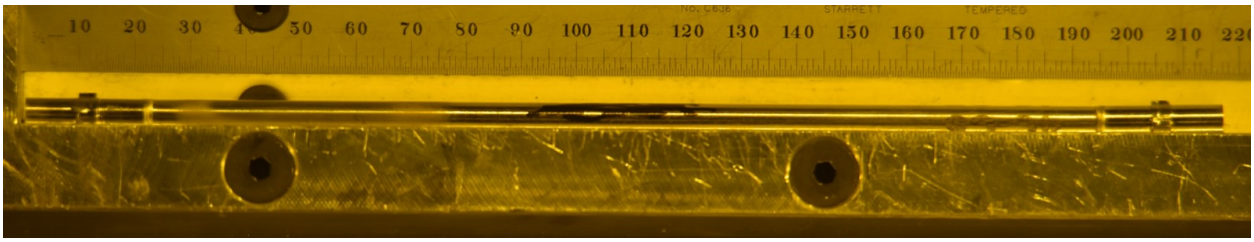

Figure 3. Visual exam photography of AFC-4C capsule 5.

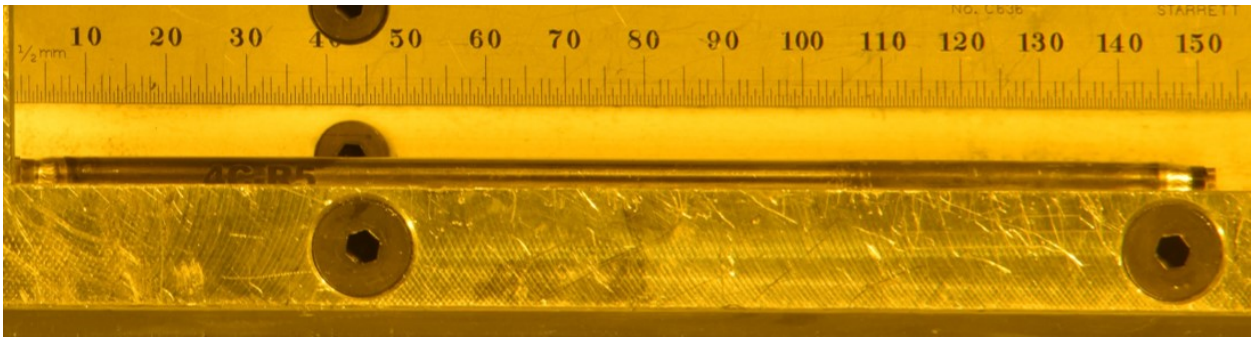

Figure 4. Visual exam photography of AFC-4C rodlet 5.

3.2 Neutron Radiography

Neutron radiography was performed using the Neutron Radiography Reactor (NRAD) located in the basement of HFEF. The NRAD reactor is a 250kW TRIGA reactor with two beam lines. The east beam line services a position below the main floor of the hot cell and is used for irradiated fuel. Neutrons pass through the fuel specimen and expose different activation foils [20]. The radiography fixture contains a scale marked with Gd paint that produces a calibrated scale for quantitative measurements of irradiated fuel dimensions. The fixture used in these shots also contained a hafnium step wedge. This allows the gray scale from radiographs to be mapped to a known neutron attenuation.

Neutron radiography images were taken of the AFC-4C-C5/R5 at 3 and 6 angles respectively with both a dysprosium (Dy) foil for thermal neutron radiography and a Cd-covered indium (In) foil for epithermal neutron radiography. For the capsule, the radiographies were taken every 120° degree using the AFC capsule carrier. For the rodlet, each angle was taken 30° apart. The rotations were fixed by placing the rodlets in a collet to fix the radial position. The collets were geared so that the fuel rodlet could be rotated exactly 30° between each shot.

An example of the thermal and epithermal neutron radiography for both capsule and rodlet 5 is shown in Figure 5. No particular features can be noticed in the capsule radiography, capsule and rodlet do not show anything unusual, and the fuel column seems to have retained dimension and geometry.
The rodlet appears to have performed well, in line with historical expectations. There are notable features in the neutron radiography of the rodlet. A region of low-density material is visible on top of the fuel, and it seems to start detaching from the fuel column itself. This region has been observed previously in metallic fuel pins and has sometimes been referred to as “fluff structure;” it has never been characterized properly until recently [21].

A sodium plug above the fuel is not readily visible. In Figure 5-b with some enhanced contrast it is possible to distinguish a sodium plug close to the end of the fuel column and also in the upper part of the rodlet plenum.

The quantitative measurement generally obtained from neutron radiography of irradiated fuels is axial growth of the fuel column. For EBR-II metallic fuel experiments, axial growth of the fuel slug was usually easy to measure using neutron radiography or precision gamma scanning. These fuel slugs began irradiation at 34.3 cm long and, although the fuel sometimes looked much less dense at the top, which made identification of the exact point of the top of the fuel slug difficult, the fuel axial growth data obtained in this way were generally consistent. In contrast, the fuel segments in the ATR experiments are less than 4 cm long. This makes it very difficult to assess in a consistent way the axial growth in these short fuel column rodlets to compare to EBR-II experiments. For AFC-4C-R5, if the fluff is considered, the axial growth accounts to 19% which is higher compared to the literature for EBR-II/Integral Fast Reactor (IFR) at this burnup (~8-11%) [10]; without the fluff, the axial growth is 5%.

Furthermore, there is a lack of consensus among experts concerning how to understand the phenomenon of axial growth in metallic fuels. There is some evidence that suggests axial growth in metallic fuel may be in part an end effect that happens in close proximity to the unconstrained, free fuel surface at the top of the fuel column. For example, measured axial growths in Fast Flux Test Facility (FFTF) irradiations of metallic fuel have been noted to be less than those for identical compositions in EBR-II [22].

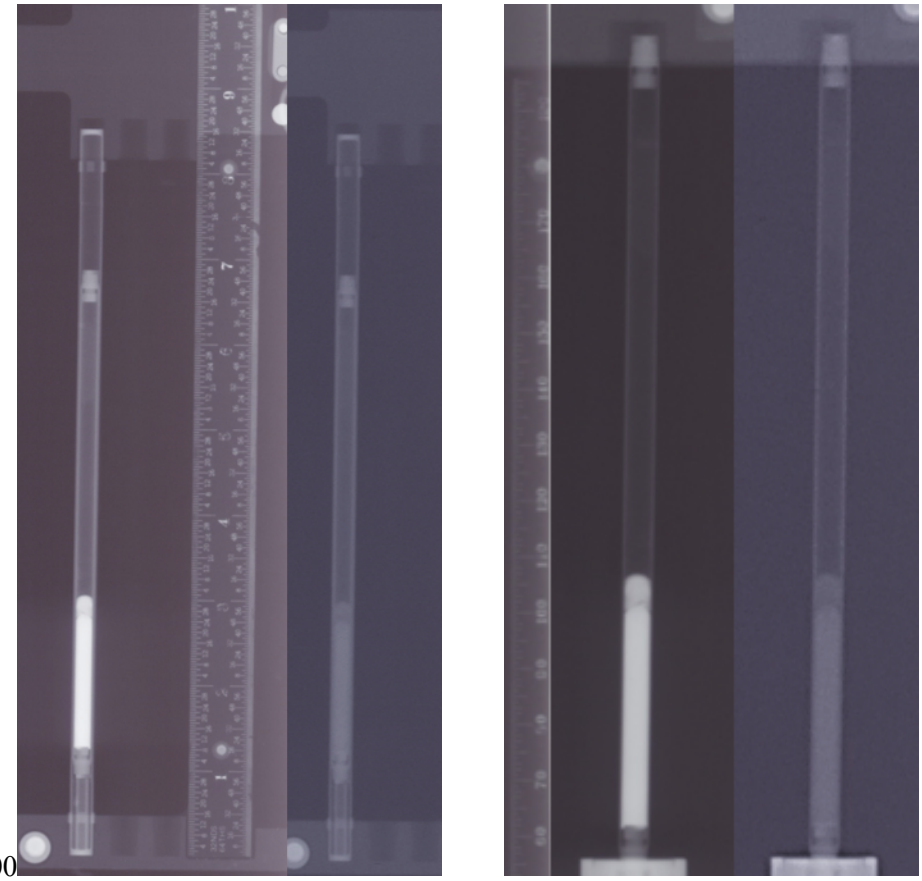

00

a) b)

Figure 5. Neutron radiography of AFC-4C-C5 (a) and -R5 (b). In both figures the thermal neutron radiography (Dy foil) is on the left and the epithermal (In foul) on the right.

3.3 Dimensional Inspection

Dimensional inspection of AFC-4C-R5 was performed using the U.S. High Performance Research Reactor (USHPRR) Plate checker in HFEF. Outside diameter measurements were collected all along the rodlets in roughly 0.5 mm increments and with two scan modalities: one scan was done at 36 angles every 5° from the initial scan angle to 180°, a second scan was done at 72 angles every 5° from the initial scan angle to 360°. Diameter measurements are collected with ±5 µm accuracy.

The 36 angles averaged measured diameters for the AFC-4C-R5 are shown in Figure 6 and, for reference, the initial cladding outer diameter is reported as a dashed red line and the capsule inner wall dimension as a green line.

The diameters are by the distance from the top of the fuel pin, which puts the fueled portion of the rodlet towards the right side of the figure. AFC-4C-R5 clearly have experienced some dimensional change in part of the fuel column (upper part of the fuel height at approx. 10-14 mm). This dimensional change accounted for a 0.6-0.8% increase in cladding diameter which is in line with the literature for this type of fuel-cladding system [10]. Because the cladding (HT-9) will not have had any void swelling, the diameter change must have been caused by creep due to fuel-cladding mechanical interaction (FCMI). It is unclear why this occurred only in this part of the fuel. When cross-sectional metallography can be performed, perhaps the reason will be found.

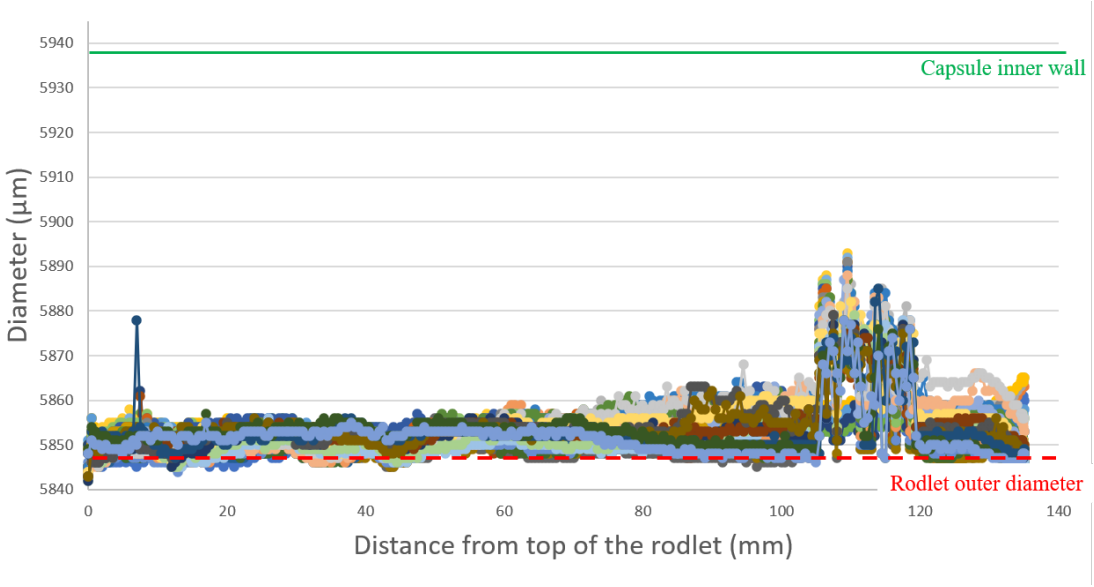

Figure 6. Diameter measurements at 36 angles for AFC-4C-R5.

3.4 Gamma Spectrometry

Gamma ray spectrometry of AFC-4C-R5 was performed using the HFEF Precision Gamma Scanner (PGS). The PGS has three major components: collimator, stage, and detector. The collimator penetrates the HFEF cell wall with a rectangular aperture that is adjustable from 0.254 cm to 0.00254 cm in height and is 2.2225 cm wide. The collimator can be rotated from a horizontal to vertical orientation. The stage manipulates the sample in front of the collimator in the plane facing the collimator and can rotate the sample about its central axis. The detector consists of a Compton suppressed high purity germanium detector, and its control system moves the stage and collimator and initiates the scans.

Several fission products were detected in the gamma spectrometry, including Ru-103/6 (as Rh-106), Sb-125, Cs-134, Cs-137, Ce-144, Eu-154, and Ce-144 (as Pr-144). Additionally, several activation products were detected, including Co-60 and Mn-54. Since Mn-54 is not a fission product, its signal is

used in the axial profile plots to indicate the location of the cladding and cladding endcaps where this signal spikes. The axial gamma spectrometry scans for the rodlet are shown in Figure 7.

The behavior of gamma emitting fission products follows trends historically observed for a solid fuel, sodium bonded [9]: Cs dissolves into the sodium and transports above the fuel column into the sodium plug located above the fuel. This also occurs with Eu-154, which tends to behave as a volatile in metallic fuel in contrast to the behavior of Ce which is tied to the behavior of the lanthanides in the fuel [23].

Ruthenium and other noble metals integrate well into metallic fuel alloys and do not migrate as shown in Figure 7.

With the superimposition of the rodlet radiography, it is possible to observe that in the "fluff structure" there are probably also non mobile fission products and fuel components as shown from the Ru-103 signal just above the fuel column with Cs-137 as well. Another peak of Eu-154 and Cs-137 is evident just at the beginning of the plenum identifying a common sodium plug. It is interesting there is another Cs-137 peak at around 11.5 cm from the bottom of the rodlet that most probably is correlated to a second (residual) sodium plug that was also mentioned in Section 3.2.

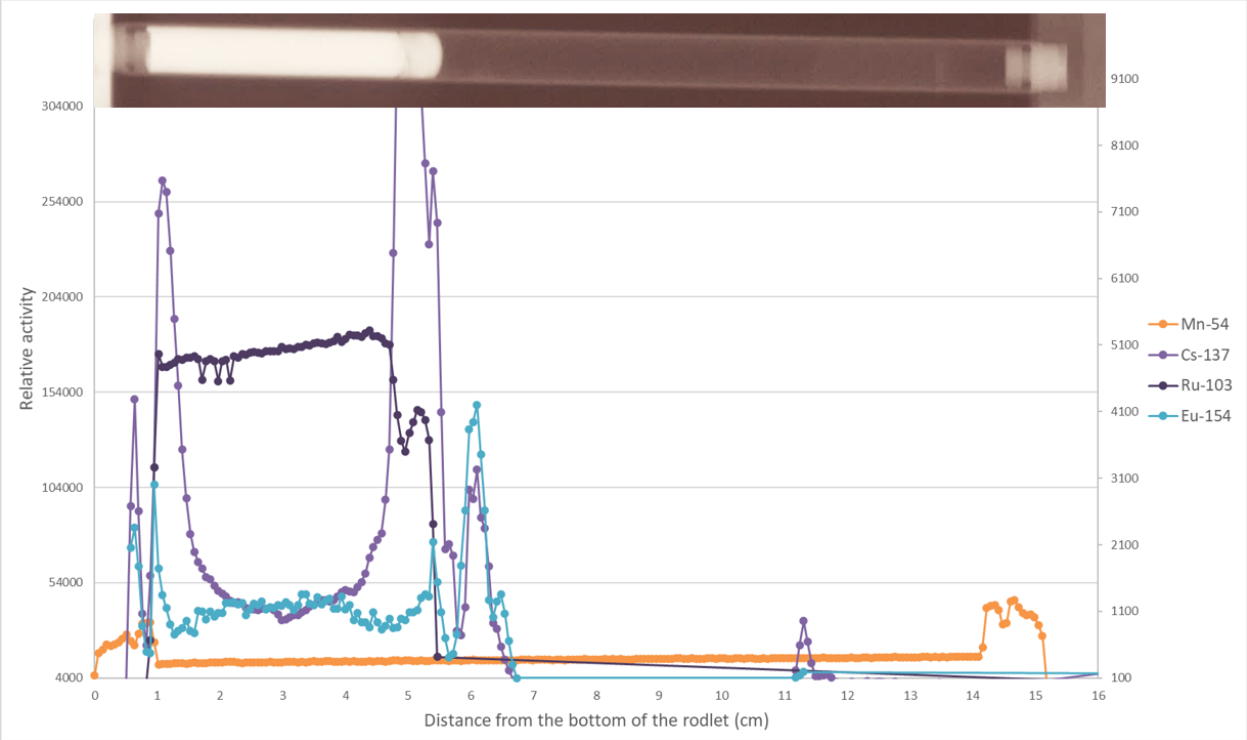

Figure 7. Axial gamma scan of AFC-4C-R5 showing key radionuclides.

4. CONCLUSIONS

The AFC-4C irradiation test investigated a variety of different fuel alloys, geometries, and bonding materials at higher burnup, compared to the lower burnup of the AFC-3 and AFC-4A series. The fuel design variations also include testing the performance of coating or barrier to mitigate FCCI. This report summarizes the non-destructive PIE performed on AFC-4C-C5/R5, a U-10Zr solid fuel, sodium bonded with HT9 cladding, Cr-coated internally, and irradiated in ATR to 8.7 at%HM burnup.

Non-destructive PIE results consist of visual exams, neutron radiography, dimensional inspection, gamma-ray spectrometry. These exams evaluated the engineering scale performance of the fuel / cladding system and, based on these results, AFC-4C-C5/R5 has behaved similar to EBR-II / IFR reference metallic fuel [6,7].

AFC-4C-R5 will continue to be examined for fission gas release analysis and more in detailed destructive examination (e.g., optical microscopy and electron microscopy) to investigate the performance of the Cr coated HT-9.

5. ACKNOWLEDGMENT

HFEF operations and process engineers are acknowledged for the different analysis and measurements performed and data acquisition. Kelly Williams, Jeff Skinner and Chris Murdock are thanked for helping to run and manage the project.

6. REFERENCES

[1] Report to Congress on the Advanced Fuel Cycle Initiative: The Future Path for Advanced Spent Fuel Treatment and Transmutation Research, (2003).
[2] S.L. Hayes, J.M. Harp, H.J.M. Chichester, R.S. Fielding, R.D. Mariani, W.J. Carmack, Advances in Metallic Fuels for High Burnup and Actinide Transmutation, in: 14th Inf. Exch. Meet. Actin. Fission Prod. Partitioning Transmutat., San Diego, CA, USA, 2016. https://doi.org/https://www.osti.gov/servlets/purl/1358285.
[3] D.C. Crawford, D.L. Porter, S.L. Hayes, Fuels for sodium-cooled fast reactors: US perspective, J. Nucl. Mater. 371 (2007) 202–231. https://doi.org/10.1016/J.JNUCMAT.2007.05.010.
[4] H.J.M. Chichester, S.L. Hayes, D. Dempsey, J.M. Harp, Advanced Reactor Fuels Irradiation Experiment Design Objectives, INL/EXT-16-39923, Rev. 0. (2016).
[5] G.L. Povirk, D. Dempsey, J.M. Harp, S.L. Hayes, Developmental Objectives for Advanced Reactor Fuels, INL/EXT-16-39923, Rev. 1. (2017).
[6] G.L. Hofman, L.C. Walters, T.H. Bauer, Metallic fast reactor fuels, Prog. Nucl. Energy. 31 (1997) 83–110. https://doi.org/10.1016/0149-1970(96)00005-4.
[7] L.C. Walters, B.R. Seidel, J.H. Kittel, Performance of Metallic Fuels and Blankets in Liquid-Metal Fast Breeder Reactors, Nucl. Technol. 65 (1984) 179–231. https://doi.org/10.13182/NT84-A33408.
[8] J.. Kittel, B.R.. Frost, J.. Mustelier, K.. Bagley, G.. Crittenden, J. Van Dievoet, History of fast reactor fuel development, J. Nucl. Mater. 204 (1993) 1–13. https://doi.org/10.1016/0022-3115(93)90193-3.
[9] W.J. Carmack, D.L. Porter, Y.I. Chang, S.L. Hayes, M.K. Meyer, D.E. Burkes, C.B. Lee, T. Mizuno, F. Delage, J. Somers, Metallic fuels for advanced reactors, J. Nucl. Mater. 392 (2009) 139–150. https://doi.org/10.1016/J.JNUCMAT.2009.03.007.
[10] T. Ogata, Metal Fuel, in: Compr. Nucl. Mater., Elsevier, 2012: pp. 1–40. https://doi.org/10.1016/B978-0-08-056033-5.00049-5.
[11] M.F. Simpson, P. Sachdev, Development of electrorefiner waste salt disposal process for the EBR-II spent fuel treatment project, Nucl. Eng. Technol. 40 (2008) 175–182.
[12] J.M. Harp, L. Capriotti, F. Cappia, Baseline Postirradiation Examination of the AFC-3C, AFC-3D, and AFC-4A Experiments, INL/EXT-18-51447. (2018).
[13] G.S. Chang, R.G. Ambrosek, Hardening neutron spectrum for advanced actinide transmutation experiments in the ATR, Radiat. Prot. Dosimetry. 115 (2005) 63–68. https://doi.org/10.1093/rpd/nci167.
[14] J.M. Harp, S.L. Hayes, P.G. Medvedev, D.L. Porter, L. Capriotti, Testing Fast Reactor Fuels in a Thermal Reactor: A Comparison Report, Idaho Natl. Lab. Rep. (2017) INL/EXT-17-41677. https://doi.org/10.2172/1458766.
[15] J.H. Kim, H.J. Ryu, J.H. Baek, S.J. Oh, B.O. Lee, C.B. Lee, Y.S. Yoon, Performance of a diffusion barrier under a fuel-clad chemical interaction (FCCI), J. Nucl. Mater. 394 (2009) 144–150. https://doi.org/10.1016/j.jnucmat.2009.08.018.
[16] S. Yeo, J.H. Kim, S.H. Eom, The characterization of electrodeposited chromium barriers for nuclear reactor cladding application, J. Nucl. Mater. 530 (2020) 151980. https://doi.org/10.1016/j.jnucmat.2019.151980.

[17] C. Woolum, R.S. Fielding, Specification for the AFC-4C Fuel Capsule Experiments in the ATR, Idaho Natl. Lab. Report, SPC-1955, Rev.1. (2015).
[18] L. Sudderth, R.S. Fielding, AFC-4C fuel as-built isotopic and chemical constituent report, Idaho Natl. Lab. Report, ECAR-3121. (2016).
[19] D. Chapman, As-Built Thermal Analysis for the AFC-3D, AFC-4B, and AFC-4C Experiments in the ATR, Idaho Natl. Lab. Rep. (2016) ECAR-3166.
[20] A.E. Craft, D.M. Wachs, M.A. Okuniewski, D.L. Chichester, W.J. Williams, G.C. Papaioannou, A.T. Smolinski, Neutron Radiography of Irradiated Nuclear Fuel at Idaho National Laboratory, in: Phys. Procedia, 2015. https://doi.org/10.1016/j.phpro.2015.07.068.
[21] F.G. Di Lemma, K.E. Wright, L. Capriotti, B.D. Miller, D.J. Murray, Microstructural Evolution of Metallic Fuel After a Power Transient, Am. Nucl. Soc. Trans. 121 (2019) 624–626.
[22] W.J. Carmack, H.M. Chichester, D.L. Porter, D.W. Wootan, Metallography and fuel cladding chemical interaction in fast flux test facility irradiated metallic U-10Zr MFF-3 and MFF-5 fuel pins, J. Nucl. Mater. 473 (2016) 167–177. https://doi.org/10.1016/j.jnucmat.2016.02.019.
[23] D.L. Porter, H. Tsai, Full-length U–xPu–10Zr (x = 0, 8, 19 wt.%) fast reactor fuel test in FFTF, J. Nucl. Mater. 427 (2012) 46–57. https://doi.org/10.1016/J.JNUCMAT.2012.03.047.